ACS NANO
Cite This: ACS Nano XXXX, XXX, XXX-XXX
www.acsnano.org

PERSPECTIVE

Perspectives for Upconverting Nanoparticles

Stefan Wilhelm*

Stephenson School of Biomedical Engineering, University of Oklahoma, 101 David L. Boren Boulevard, Norman, Oklahoma 73072, United States

ABSTRACT: **Upconverting nanoparticles (UCNPs) are inorganic crystalline nanomaterials that can convert near-infrared (NIR) excitation light into visible and ultraviolet emission light. Excitation with NIR light minimizes autofluorescence background and enables deeper penetration into biological samples due to reduced light scattering. Although these optical features make UCNPs promising candidates for bioanalytical and biomedical applications, the performance of UCNPs is compromised by their low optical brightness. Research in the field of UCNP technology focuses on strategies to boost upconversion luminescence brightness and efficiencies. In this Perspective, I discuss challenges associated with the use of UCNPs and provide a 10-year proposed strategic plan to enable translation of UCNP technology from the academic stage into real world products and applications.**

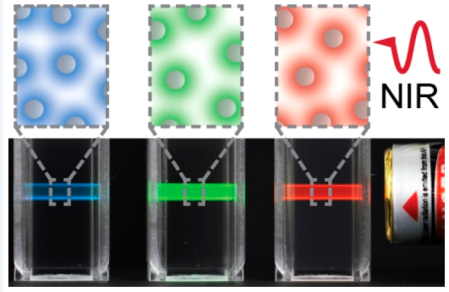

Upconverting nanoparticles (UCNPs) are a class of luminescent nanomaterials with the fascinating ability to emit light with shorter wavelength than the excitation light. This photophysical phenomenon is based on an anti-Stokes process and referred to as photon upconversion; that is, sequential absorption of two or more low-energy photons to populate real, intermediate excited electronic states followed by emission of a single high-energy photon (Figure 1a–d). The origin of this research field goes back to the year 1959, when Bloembergen introduced the idea of ion-doped solid-state infrared quantum counters. This was followed by experimental work from Auzel, Ovsyankin, and Feofilov in the mid-1960s.[1] While early studies in this research area focused on rare-earth ion-doped glassy and crystalline upconverting bulk materials, increasing effort has been dedicated to upconversion nanomaterials, *i.e.*, UCNPs, in the past 10 years.

Upconverting nanoparticles can be synthesized with defined physicochemical properties (*e.g.*, size, shape, and surface chemistry). Typical examples of UCNPs include inorganic nanoparticles based on a $NaYF_4$ crystalline host matrix that contains a combination of upconversion sensitizer (*e.g.*, Yb^{3+}) and activator (*e.g.*, Er^{3+} and Tm^{3+}) lanthanide ions (Figure 1a–e). Upon excitation with near-infrared (NIR) continuous wave laser light, these types of UCNPs display anti-Stokes shifted visible and ultraviolet emission with minimal autofluorescence background. These optical properties make UCNPs attractive candidates for a variety of broad applications, including sensing, imaging, diagnosis, and therapy, as well as photovoltaic, security, and display technology. Despite the tremendous potential that UCNPs offer for these types of applications, a number of limitations still need to be addressed. In this Perspective, I provide a discussion of challenges that UCNPs face and highlight opportunities and future directions for the field.

One of the greatest trends and, at the same time, major challenges in the field of upconverting nanoparticle research is the quest to enhance upconversion luminescence.

Enhancing Upconversion Luminescence. Due to their unique optical properties, UCNPs have been considered promising alternatives for conventional luminophores, such as organic dyes and semiconductor quantum dots. However, in comparison to conventional luminophores, quantum yields of lanthanide-doped UCNPs are relatively low (typically <1%) and, in general, about an order of magnitude lower than those of corresponding upconversion bulk materials (Table 1). Hence, one of the greatest trends and, at the same time, major challenges in the field of UCNP research is the quest to enhance upconversion luminescence.

Upconversion luminescence of UCNPs involves nonlinear photophysical processes through sequential absorption of excitation photons by sensitizer lanthanide ions and energy transfer to activator ions (Figure 1c,d). Consequently, optical properties of UCNPs (*e.g.*, luminescence intensity and quantum yield) are excitation power (P)-dependent, and saturation effects occur upon increasing the excitation power density as shown in Figure 1f for the absolute quantum yield of UCNPs.[2] The P-dependent quantum yield of UCNPs is defined by eq 1:

$$QY_{UC}(P) = \frac{N_{em}}{N_{abs}} \quad \text{for} \quad \lambda_{em} < \lambda_{abs} \tag{1}$$

DOI: 10.1021/acsnano.7b07120
ACS Nano XXXX, XXX, XXX–XXX

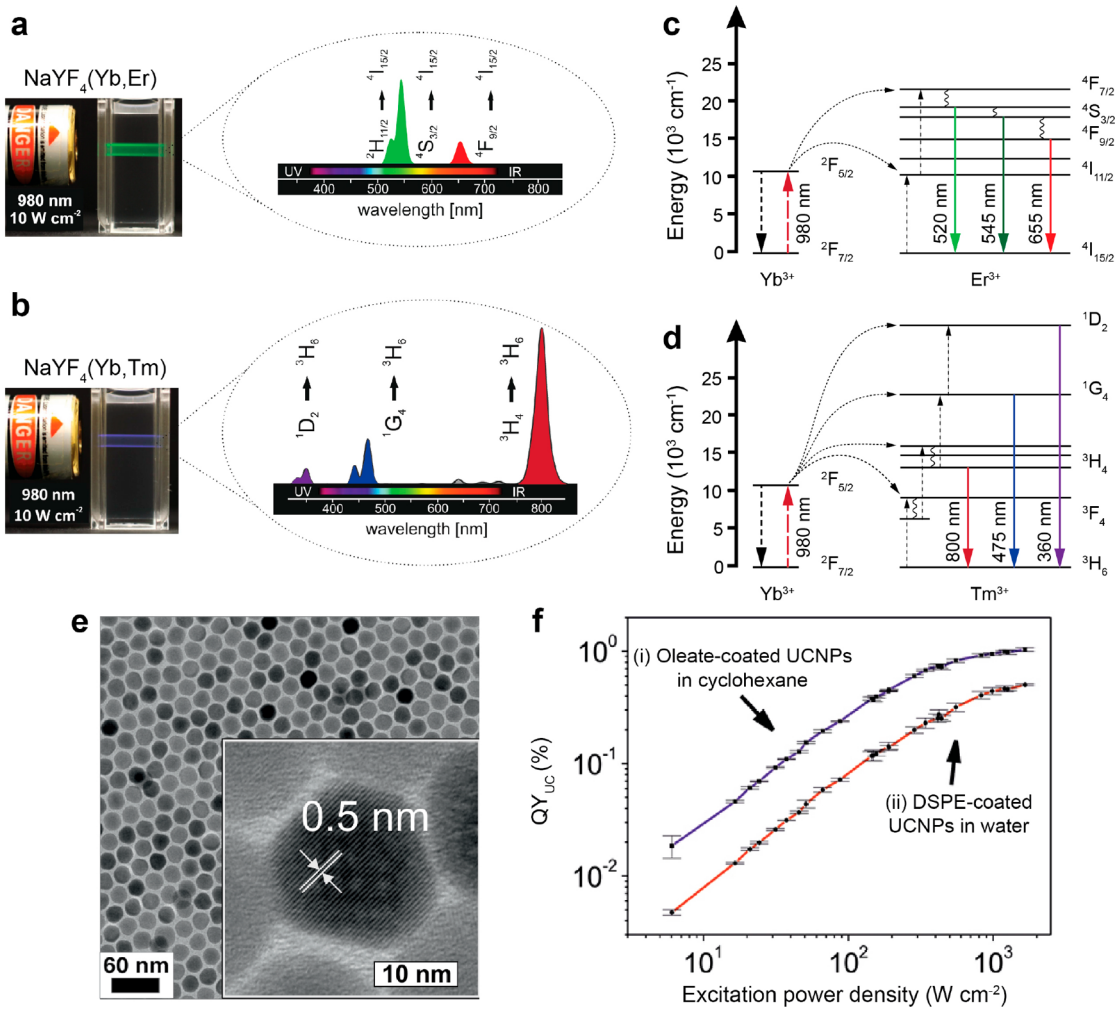

Figure 1. Photophysical and physicochemical properties of upconverting nanoparticles (UCNPs). Colloidal dispersions of (a) oleate-coated hexagonal phase β-$NaYF_4(Yb^{3+}/Er^{3+})$ UCNPs and (b) β-$NaYF_4(Yb^{3+}/Tm^{3+})$ UCNPs in cyclohexane with corresponding upconversion luminescence spectra upon 980 nm continuous wave (CW) laser excitation (10 W/cm^2). Simplified energy level diagrams and energy transfer upconversion mechanisms for (c) Yb^{3+}/Er^{3+}-doped and (d) Yb^{3+}/Tm^{3+}-doped sensitizer/activator ion systems. Excitation light (980 nm) is absorbed by Yb^{3+} sensitizer ions and sequentially transferred to Er^{3+}/Tm^{3+} activator ions. Arrows indicate radiative, nonradiative energy transfer, and multiphonon relaxation processes. (e) Transmission electron (TEM) micrograph of β-$NaYF_4(Yb^{3+}/Er^{3+})$ UCNPs (Inset: high-resolution TEM image of single UCNP with characteristic crystal lattice fringes). Nanoparticle diameter = 22.7 ± 0.7 nm. Reproduced with permission from ref 8. Copyright 2015 Royal Society of Chemistry. (f) Power density-dependent absolute upconversion luminescence quantum yield (QY_{UC}) of UCNPs shown in (e) upon 976 nm CW laser excitation. (i) Hydrophobic oleate-coated β-$NaYF_4(Yb^{3+}/Er^{3+})$ UCNPs dispersed in cyclohexane and (ii) hydrophilic DSPE-coated β-$NaYF_4(Yb^{3+}/Er^{3+})$ UCNPs dispersed in water. DSPE, 1,2-distearoyl-*sn*-glycero-3-phosphoethanolamine-*N*-[methoxy-(poly ethylene glycol)-2000] (ammonium salt).

where N_{em} is the number of upconversion photons emitted and N_{abs} is the number of photons absorbed at the excitation wavelength (for example, 980 nm) for a given laser excitation power density.[3] In the past 5−10 years, researchers have aimed at synthesizing small UCNPs (<10 nm in diameter) with narrow size distributions and colloidal stability in biologically relevant media and buffer systems.[4−7] As shown in Table 1, the quantum yields of UCNPs decrease significantly with decreasing nanocrystal diameter for a given laser excitation power density. Interestingly, the quantum yields of UCNPs with exactly the same size (obtained from the same synthesis batch) depend on the surface ligand coating and dispersion medium for a given excitation power density (Table 1).[3,8] These findings suggest that there are many factors that contribute to the low upconversion luminescence efficiency of UCNPs. Table 2 provides examples of these parameters classified into three broad categories: (i) nanoparticle, (ii) surface chemistry, and (iii) dispersion medium. A detailed discussion of these parameters is beyond the scope of this Perspective, and the reader is referred to excellent review articles on this topic.[9−12]

Strategies to increase the upconversion luminescence efficiency have been reviewed by Liu *et al.* and are schematically summarized in Figure 2a.[10] An effective and commonly used strategy to boost upconversion luminescence efficiency is surface passivation by synthesizing core−shell nanocrystals.[13] Surface passivation minimizes luminescence quenching through surface effects by (i) shielding lanthanide ions at the nanoparticle surface with a protective shell and (ii) reducing nanocrystal surface defects. Ideally, these passivation shells should be isotropic with no intermixing of lanthanide dopant ions from the core nanocrystal and the shell material. Alivisatos and co-workers published a systematic study in 2016 on how shell thickness of β-$NaYF_4(Yb/Er)$@β-$NaLuF_4$ core−shell

DOI: 10.1021/acsnano.7b07120
ACS Nano XXXX, XXX, XXX−XXX

Table 1. Examples of Upconversion Luminescence Quantum Yields of Different Types of Bulk Upconversion Materials and Upconverting Nanoparticles[a]

material composition and doping concentrations (mol %)	crystal phase	nanoparticle type	nanoparticle size (nm)	wavelength (nm)	power density (W cm^{-2})	quantum yield (%)	surface ligand	dispersion medium	method used for quantum yield measurement	ref
La_2O_2S/Yb/Er (1:1)	hexagonal	n/a	5−7 μm bulk material	980	22	6.20 ± 0.90	n/a	n/a	absolute; integrating sphere setup	31
					19	5.50 ± 0.80				
La_2O_2S/Yb/Er (3:7)	hexagonal	n/a	5−7 μm bulk material	980	16	5.10 ± 0.76	n/a	n/a	absolute; integrating sphere setup	31
					9	4.20 ± 0.60				
La_2O_2S/Yb/Er (0:1)	hexagonal	n/a	5−7 μm bulk material	980	19	4.44 ± 0.66	n/a	n/a	absolute; integrating sphere setup	31
La_2O_2S/Yb/Er (2:8)	hexagonal	n/a	5−7 μm bulk material	980	16	3.60 ± 0.50	n/a	n/a	absolute; integrating sphere setup	31
La_2O_2S/Yb/Er (9:1)	hexagonal	n/a	4−6 μm bulk material	977	13	5.8 ± 0.9	n/a	n/a, measured in powder form	absolute; integrating sphere setup	32
					3.8	4.87 ± 0.70				
					0.5	0.40 ± 0.06				
$NaYF_4$/Yb/Er (20:2)	hexagonal	n/a	4 ± 1 μm bulk material	977	22	7.8 ± 1.2	n/a	n/a, measured in powder form	absolute; integrating sphere setup	32
					3.8	1.7 ± 0.3				
					0.5	0.21 ± 0.03				
$NaYF_4$/Yb/Er (20:2)	hexagonal	n/a	≫100 bulk material	980	20	3.0 ± 0.3	n/a	n/a	absolute; integrating sphere setup	33
$NaYF_4$/Yb/Er (18:2)	hexagonal	n/a	0.5 mm powders of 600 and 1000 μm fibers bulk material	980	∼20 power density varied from <0.1 to ∼1000	∼4	n/a	n/a, measured in powder form	absolute; integrating sphere setup	34
$NaYF_4$/Yb/Er (20:2)	hexagonal	core only	100	980	150	0.30 ± 0.10	oleate	hexane	absolute; integrating sphere setup	33
$NaYF_4$/Yb/Tm (25:0.3)	hexagonal	core only	38	975	3.8 power density varied from 0.027 to 20	0.45 (UC emission band at 800 nm)	oleate	hexane	relative; system employed standard fluorophores calibrated using the integrating-sphere based Hamamatsu C9920 quantum yield measurement system	35
$NaYF_4$/Yb/Er (20:2)	hexagonal	core only	37	980	10^3	0.14 ± 0.01	oleate	hexane	absolute; integrating sphere setup	6
$NaYbF_4$/Tm 0.5 for Tm	hexagonal	core only with IR-808 dye sensitizer (no. of dye molecules per nanoparticle n/a)	33	∼800	12.5	∼3.1	IR-808 dye	dimethylformamide	relative; referenced to indocyanine green in DMSO with quantum yield of 12%	13
$NaYF_4$/Yb/Er (20:2)	hexagonal	core only	30	980	150	0.10 ± 0.05	oleate	hexane	absolute; integrating sphere setup	33
$LiLuF_4$/Yb/Tm (20:0.5)	tetragonal	core only	28	980	127	0.61	oleate	cyclohexane	absolute; integrating sphere setup	36
$LiLuF_4$/Yb/Er (20:1)	tetragonal	core only	28	980	127	0.11	oleate	cyclohexane	absolute; integrating sphere setup	36
$NaYF_4$/Yb/Er (33:5)	hexagonal	core only	∼24	980	63 power density varied from ∼1 to ∼63	0.07 ± 0.01	oleate	chloroform	absolute; integrating sphere setup	14
$NaYF_4$/Yb/Er (20:2)	hexagonal	core only	22.7	976	150 power density varied from 10 to 1000	∼0.4	amphiphilic coating w/oleate and DSPE	deuterium oxide	absolute; integrating sphere setup	3
$NaYF_4$/Yb/Er (20:2)	hexagonal	core only	22.7	976	150 power density varied from 10 to 1000	∼0.35	BF_4^-	dimethylformamide	absolute; integrating sphere setup	3
$NaYF_4$/Yb/Er (20:2)	hexagonal	core only	22.7	976	150	∼0.35	oleate	cyclohexane	absolute; integrating sphere setup	8

DOI: 10.1021/acsnano.7b07120
ACS Nano XXXX, XXX, XXX−XXX

Table 1. continued

material composition and doping concentrations (mol %)	crystal phase	nanoparticle type	nanoparticle size (nm)	wavelength (nm)	power density (W cm^{-2})	quantum yield (%)	surface ligand	dispersion medium	method used for quantum yield measurement	ref
$NaYF_4$/Yb/Er (20:2)	hexagonal	core only	22.7	976	150 power density varied from 6 to 1600	~0.1	amphiphilic coating w/ oleate and DSPE	water	absolute; integrating sphere setup	37
$NaYF_4$/Yb/Er (20:2)	hexagonal	core only	22.7	976	150 power density varied from 10 to 1000	~0.1	citrate	water	absolute; integrating sphere setup	3
$NaYF_4$/Yb/Er (20:2)	hexagonal	core only	8−10	980	150	0.005 ± 0.005	oleate	hexane	absolute; integrating sphere setup	33
$NaYF_4$/Yb/Er (2:20)	hexagonal	core only	8	976	100	1.5×10^{-2}	oleate	hexane	absolute; integrating sphere setup	4
$NaYF_4$/Yb/Er (20:2)	hexagonal	core only	8	976	100	1.1×10^{-2}	oleate	hexane	absolute; integrating sphere setup	4
$NaYF_4$/Yb/Er/Gd (20:2:25)	hexagonal	core only	8	976	100	6.3×10^{-4}	oleate	hexane	absolute; integrating sphere setup	4
$NaLuF_4$:Gd/Yb/Tm (24:20:1)	hexagonal	core only	7.8	980	17.5	0.47 ± 0.06	n/a	n/a	absolute; integrating sphere setup	38
$NaYF_4$/Yb/Er (20:2)	hexagonal	core only	5.4	980	10^3	0.0022 ± 0.0001	oleate	hexane	absolute; integrating sphere setup	6
$NaGdF_4$/Yb/Er (20:2)	hexagonal	core only	5	980	100	0.02 ± 0.08	oleate	cyclohexane	absolute; integrating sphere setup	39
$NaYF_4$/Yb/Er (0:20)	hexagonal	core only	5	976	100	1.2×10^{-2}	oleate	hexane	absolute; integrating sphere setup	4
$NaYF_4$/Yb/Er (20:2)	hexagonal	core only	5	976	100	2.2×10^{-3}	oleate	hexane	absolute; integrating sphere setup	4
$NaYF_4$/Yb/Er/Gd (20:2:25)	hexagonal	core only	5	976	100	7.2×10^{-4}	oleate	hexane	absolute; integrating sphere setup	4
$NaYbF_4$/Tm@$NaYF_4$/Nd 0.5 for Tm; 30 for Nd	hexagonal	core−shell with IR-808 dye sensitizer (830 dyes per nanoparticle)	51 core: 33 shell: 18	~800	10 power density varied from ~1 to ~14	~4.8	IR-808 dye	dimethylformamide	relative; referenced to indocyanine green in DMSO with quantum yield of 12%	13
$LiLuF_4$/Yb/Tm@$LiLuF_4$ (20:0.5)	tetragonal	core−shell	50 core: 28 shell: 22	980	127	7.6	oleate	cyclohexane	absolute; integrating sphere setup	36
$LiLuF_4$/Yb/Er@$LiLuF_4$ (20:1)	tetragonal	core−shell	50 core: 28 shell: 22	980	127	5.0	oleate	cyclohexane	absolute; integrating sphere setup	36
$NaYF_4$/Yb/Er@$NaLuF_4$ (33:5)	hexagonal	core−shell	~50 core: ~24 shell: ~13	980	63 power density varied from ~1 to ~63	4 ± 0.5	oleate	chloroform	absolute; integrating sphere setup	14
$LiLuF_4$/Yb/Tm@$LiLuF_4$ (20:0.5)	tetragonal	core−shell	40 core: 28 shell: 12	980	127	6.7	oleate	cyclohexane	absolute; integrating sphere setup	36
$LiLuF_4$/Yb/Er@$LiLuF_4$ (20:1)	tetragonal	core−shell	40 core: 28 shell: 12	980	127	3.6	oleate	cyclohexane	absolute; integrating sphere setup	36
$NaYF_4$/Yb/Tm@$NaYF_4$ (20:0.3)	hexagonal	core−shell	43 core: 31 shell: 12	975	78 power density varied from 0.027 to 80	3.5 (UC emission band at 800 nm)	oleate	hexane	relative; system employed standard fluorophores calibrated using the integrating-sphere based Hamamatsu C9920 quantum yield measurement system	40
$NaYF_4$/Yb/Tm@$NaYF_4$ (20:0.3)	hexagonal	core−shell	43 core: 33 shell: 10	975	1.3 power density varied from 0.027 to 20	1.2 (UC emission band at 800 nm)	oleate	hexane	relative; system employed standard fluorophores calibrated using the integrating-sphere based Hamamatsu C9920 quantum yield measurement system	35

DOI: 10.1021/acsnano.7b07120
ACS Nano XXXX, XXX, XXX−XXX

Table 1. continued

material composition and doping concentrations (mol %)	crystal phase	nanoparticle type	nanoparticle size (nm)	wavelength (nm)	power density (W cm^{-2})	quantum yield (%)	surface ligand	dispersion medium	method used for quantum yield measurement	ref
$NaYF_4$/Yb/Er@$NaYF_4$ (20:2)	hexagonal	core–shell	30 core: 20 shell: 10	980	150	0.30 ± 0.10	oleate	hexane	absolute; integrating sphere setup	33
$NaYbF_4$/Tm@CaF_2 0.5 for Tm	cubic	core–shell	27 core: 20 shell: 7	975	0.3	0.6 ± 0.1	oleate	hexane	relative; referenced to standard: IR-26 dye dissolved in 1,2-dichloroethane, with a known QY of 0.05%	41
$NaGdF_4$/Yb/Er@$NaYF_4$ (20:2)	hexagonal	core–shell	17 core: 5 shell: 12	980	100	0.51 ± 0.08	oleate	cyclohexane	absolute; integrating sphere setup	39
$NaYF_4$/Yb/Er@$NaYF_4$ (20:2)	hexagonal	core–shell	11 core: 8 shell: 3	976	100	0.49	oleate	hexane	absolute; integrating sphere setup	4
$NaYF_4$/Yb/Er@$NaYF_4$ (20:2)	hexagonal	core–shell	9 core: 5.4 shell: 3.6	980	10^3	0.18 ± 0.01	oleate	hexane	absolute; integrating sphere setup	6

[a]Abbreviations: DSPE, 1,2-distearoyl-*sn*-glycero-3-phosphoethanolamine-*N*-[methoxy-(poly ethylene glycol)-2000] (ammonium salt); DMSO, dimethylsulfoxide.

UCNPs affects the upconversion luminescence quantum yield (QY_{UC}). The shell thickness around ∼24 nm core β-$NaYF_4$(Yb/Er) UCNPs was systematically increased in 10 steps from ∼0.3 to ∼13 nm. The QY_{UC} of core only UCNPs could be improved from ∼0.07 to ∼4% for core–shell UCNPs with a shell thickness of ∼13 nm (excitation power density of 63 W/cm^2 at 980 nm). This study further showed that QY_{UC} did not change significantly for core–shell UCNPs once the shell thickness was >4 nm.[14]

While core–shell architectures are an elegant way to increase upconversion luminescence efficiency, this strategy might limit the use of UCNPs for Förster resonance energy transfer (FRET)-based applications. The thickness of the passivation shell has to be optimized to reach a compromise between upconversion luminescence enhancement and donor–acceptor distance-dependent FRET efficiency, as shown in a study by Hirsch and co-workers.[15] A different but remarkable strategy to improve upconversion luminescence intensity was reported by Li *et al.* in this issue of *ACS Nano*.[16] Here, a living yeast cell was optically trapped by a fiber probe to focus the 980 nm laser excitation light. The yeast cell was used as a biomicrolens to generate a photonic nanojet for the excitation of ∼28 nm β-$NaYF_4$(Yb/Tm)@Silica core–shell UCNPs. Authors reported an enhancement of upconversion luminescence intensity of approximately 2 orders of magnitude when using the yeast cell biomicrolens approach for excitation (Figure 2b–e).

> A remarkable strategy to improve upconversion luminescence intensity was reported by Li *et al.* in this issue of *ACS Nano*.

The examples by the groups of Alivisatos and Li show that upconversion luminescence can be enhanced by different strategies, including (i) material design, (ii) engineering of the excitation source, or (iii) a combination of both parameters. In addition, the work by Li *et al.* emphasizes that low upconversion luminescence efficiencies and QY_{UC} can be limiting factors and potentially exclusion criteria for certain applications of UCNPs.[16] Hence, there is a clear need for the research community to find innovative methods for upconversion luminescence enhancement and brighter UCNPs. It is worth mentioning that, for some applications, absolute signal intensities and luminescence efficiencies are less important than signal-to-noise ratio. Because NIR light is used for the excitation of UCNPs, the minimal autofluorescence background can provide an attractive signal-to-noise ratio. Consequently, detection limits of UCNP emission light may be orders of magnitude better than those achieved with ultraviolet-excitable quantum dots. In addition to the enhancement of upconversion luminescence efficiency (that is, QY_{UC}), the brightness of UCNPs can be further enhanced by increasing their molar attenuation coefficient (or absorption cross section) at the excitation wavelength. The brightness (B) of UCNPs is defined by eq 2:

$$B_{UC} = \varepsilon(\lambda_{ex})QY_{UC}(P) \quad (2)$$

where $\varepsilon(\lambda_{ex})$ is the molar attenuation coefficient at the excitation wavelength and $QY_{UC}(P)$ is the P-dependent upconversion luminescence quantum yield.[17] Increasing the

DOI: 10.1021/acsnano.7b07120
ACS Nano XXXX, XXX, XXX–XXX

Table 2. Examples of Key Parameters That Affect Upconversion Luminescence Efficiency of Upconverting Nanoparticles

category	parameter
nanoparticle	nanoparticle diameter
	(i) surface area to volume ratio increases with decreasing nanoparticle diameter (d); $6d^{-1}$
	(ii) as the nanoparticle diameter decreases, an increasing number of ions are located at the particle surface
	(iii) higher chances for reduction of upconversion luminescence by surface quenching effects
	crystal host material and crystal phase
	(i) long lifetimes of excited electronic states are favorable and a prerequisite for sequential absorption of low-energy photons
	(ii) fluoride-based host materials (*e.g.*, $NaYF_4$) exhibit relatively low phonon energies (~350 cm^{-1}), beneficial for providing long lifetimes of excited electronic states
	(iii) hexagonal crystal phase of $NaYF_4$ provides higher upconversion luminescence efficiency than cubic phase
	(iv) crystal lattice impurities and defects may increase nonradiative multiphonon relaxation rates
	lanthanide ion dopants
	(i) number of dopant ions determines their inter-ion distance
	(ii) increased changes for cross relaxation processes resulting in luminescence quenching with increasing dopant concentrations
	(iii) light-harvesting ability of lanthanide ions is limited due to low molar extinction coefficients, for example, $\varepsilon(Yb^{3+})_{980\ nm}$ = ~10 $M^{-1}\ cm^{-1}$
surface chemistry	surface ligands and coatings with high-energy vibrational modes that match energy differences between numerous energy levels of lanthanide dopant ions, including
	(i) O−H (~3200−3700 cm^{-1})
	(ii) N−H (~3300−3500 cm^{-1})
	(iii) C−H (~2800−2950 cm^{-1})
dispersion medium	dispersion media with high-energy vibrational modes, including O−H, N−H, C−H
	dispersion media with high extinction coefficients at the upconversion luminescence excitation wavelength, for example, H_2O (absorption coefficient at 980 nm = ~0.485 cm^{-1})

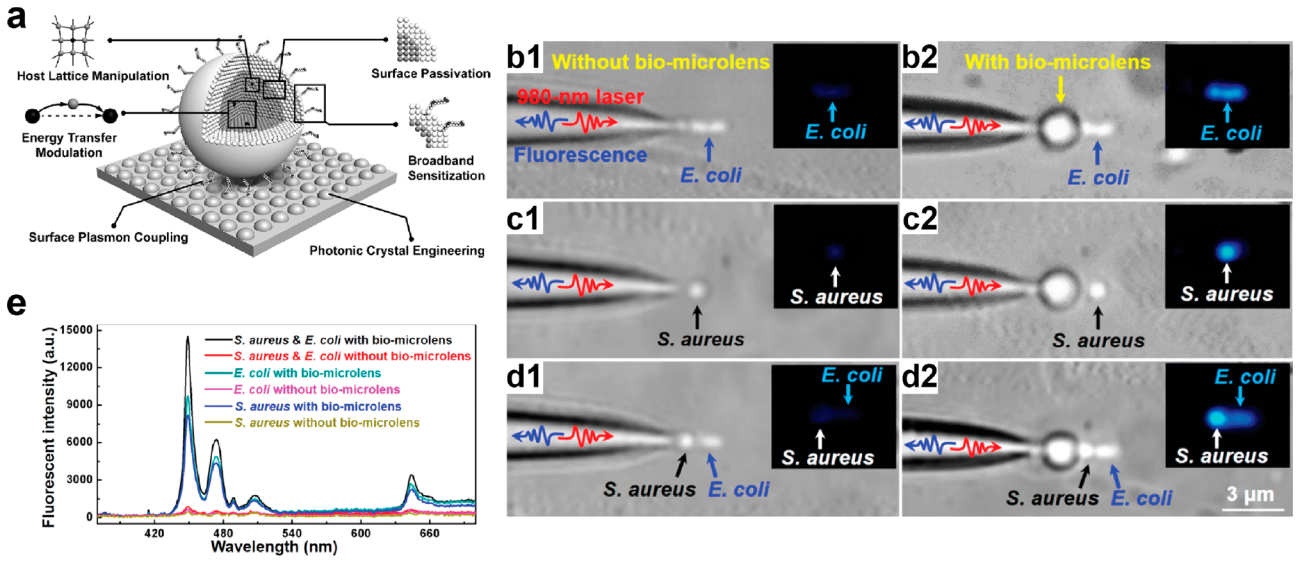

Figure 2. Strategies for enhancing upconversion luminescence of upconverting nanoparticles (UCNPs). (a) Schematic overview of main strategies for enhancing upconversion luminescence of lanthanide-doped UCNPs. These strategies may be combined to achieve synergistic upconversion luminescence enhancement. (b−e) Use of a biomicrolens to enhance upconversion luminescence. (b1−d1) Optical micrographs of single (b1) *Escherichia coli*, (c1) *Staphylococcus aureus*, and (d1) *S. aureus* and *E. coli* labeled with 28 nm $NaYF_4(Yb^{3+}/Tm^{3+})$@ silica core−shell UCNPs optically trapped by an optical fiber probe without and with (b2−d2) a 2 μm yeast cell biomicrolens. (e) Corresponding upconversion luminescence spectra. Adapted with permission from refs 10 and 16. Copyrights 2014 John Wiley and Sons and 2017 American Chemical Society, respectively.

values of $\varepsilon(\lambda_{ex})$ or $QY_{UC}(P)$ (or both photophysical parameters) can boost the brightness of UCNPs.[11]

Engineering Colloidal Stability and Excitation Wavelength of Upconverting Nanoparticles. The majority of biological applications of colloidal UCNPs requires aqueous buffer systems. This can create problems for the use of UCNPs from two different aspects. First, the synthesis of high-quality colloidal UCNPs is typically carried out in organic solvents with relatively high boiling points (*e.g.*, mixtures of 1-octadecene and oleic acid). Through the adsorption of hydrophobic organic molecules onto the nanoparticle surface during synthesis, UCNPs are only dispersible in nonpolar solvents. Thus, surface modification strategies are required to render UCNPs hydrophilic and colloidally stable in water and buffer systems.[18] Although systematic studies have been performed in recent years to address this challenge, there is still a need to develop simple and robust ligand exchange and amphiphilic coating procedures to increase colloidal stability of UCNPs in aqueous buffer systems, such as phosphate buffered media.[8,19,20] Because QY_{UC} and brightness (B_{UC}) of UCNPs are typically low,

DOI: 10.1021/acsnano.7b07120
ACS Nano XXXX, XXX, XXX−XXX

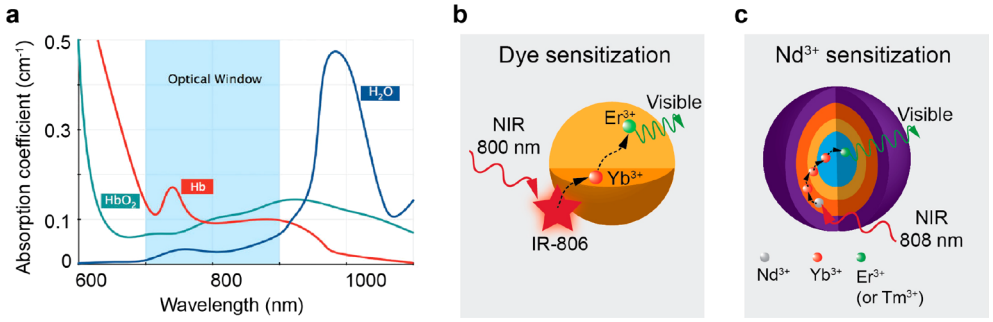

Figure 3. Strategies for engineering the excitation wavelength of upconverting nanoparticles (UCNPs). (a) Absorption spectra of major light absorbers in biological tissue, *i.e.*, hemoglobin and water. Absorption of water at 800 nm is significantly reduced in comparison to 980 nm. (b,c) Schematics highlighting strategies to shift the excitation wavelength from 980 to 800 nm with (b) near-infrared (NIR) dye IR-806 sensitized upconversion and (c) Nd^{3+} sensitized upconversion. Adapted with permission from refs 25 and 30. Copyrights 2016 John Wiley and Sons and 2010 Nature Publishing Group, respectively.

relatively high nanoparticle concentrations are required to achieve reasonable signal readouts, for example, in bioanalytical assays.[21] Therefore, surface modifications are needed that (i) enable colloidal stability at high nanoparticle concentrations and (ii) exhibit chemical functional groups for further modification and bioconjugation.

Second, the typical excitation wavelength for UCNPs based on Yb^{3+}/Er^{3+} (or Tm^{3+}) sensitizer/activator ion systems is 980 nm. This wavelength matches the energy difference between Yb^{3+} sensitizer ion's $^2F_{7/2}$ and $^2F_{5/2}$ electronic states (Figure 1c,d). However, the excitation wavelength of UCNPs overlaps with the local absorption maximum of water located at ~980 nm (absorption coefficient of ~0.485 cm^{-1}; Figure 3a). The consequence is that excitation of colloidal UCNPs in water can cause severe overheating. The increase in temperature upon excitation with 980 nm laser light may be problematic for *in vitro* tissue culture as well as *in vivo* bioanalytical and biomedical applications.[22] Strategies have been developed in the last 5 years to shift the excitation wavelength for UCNPs from 980 nm to approximately 800 nm, where the absorption of water is significantly reduced (Figure 3a). The first strategy is to coat the UCNP surface with organic dyes, such as IR-806. This dye absorbs NIR light broadly with an absorption maximum at ~806 nm and enables subsequent energy transfer to Yb^{3+} sensitizer ions of β-$NaYF_4$(Yb/Er) UCNPs to excite upconversion luminescence (Figure 3b). Hummelen and co-workers showed that this approach enables a shift in the excitation wavelength to the more favorable 800 nm range; they also reported that the integrated upconversion luminescence intensity could be increased by a factor of ~3300 using IR-806 dye-modified UCNPs in comparison to unmodified UCNPs.[23] Shortcomings of these dye-modified UCNP systems include (i) limited photostability of NIR organic dyes and (ii) the need for additional phase transfer and surface modification steps to make them dispersible in water and aqueous buffers. A second strategy to shift the excitation wavelength of UCNPs to the 800 nm range exploits the use of Nd^{3+} ions as cosensitizers for Yb^{3+}/Er^{3+} (or Tm^{3+})-doped UCNPs (Figure 3c).[24,25] Neodymium(III) ions absorb laser excitation light with a wavelength of ~808 nm and can sequentially transfer the excitation energy to Yb^{3+} sensitizer ions through energy transfer mechanisms. This cascade sensitization process requires sophisticated core–shell and core–multishell architectures to enhance upconversion luminescence efficiency by spatially separating Nd^{3+} sensitizer and Er^{3+}/Tm^{3+} activator ions. Dye sensitization can be combined with Nd^{3+} sensitization as recently demonstrated by Prasad and co-workers.[13,26] These strategies not only shift the excitation wavelength to a more favorable spectral region but also increase the brightness of UCNPs by improving $\varepsilon(\lambda_{ex})$ and/or $QY_{UC}(P)$. These enhancements open new opportunities for the use of UCNPs in a variety of applications, including bioimaging, photovoltaics, and multicolor display technologies.

PERSPECTIVES AND OUTLOOK

The field of upconversion luminescence research continues to grow. Nanotechnology contributed significantly to growth and development in this field with increasing focus on synthesis, characterization, and application of UCNPs. The interest in UCNP research reflects the potential that nanotechnology offers for the field of upconversion luminescence.

With the advances in material synthesis in the early and mid-2000s, it was possible to fabricate high quality and monodisperse UCNPs through bottom-up synthesis procedures. This development opened up new possibilities for applications of UCNPs in the bioanalytical and biomedical fields. The concept of minimizing autofluorescence background with UCNP-based labels and probes upon NIR light excitation seemed intriguing at the academic stage and has fueled research in this field. The goal for the next ten years can be summarized by a single key word: translation. Research on UCNPs has to demonstrate that it can evolve from the academic setting into real world products and applications. To help advance this progress, a strategic plan is proposed in Figure 4. Iterative processes between basic studies and application and development stages will be necessary with clearly defined objectives and aims. Synthesis and surface modification of UCNPs are at the very core of this process. The quality of UCNPs has to be thoroughly characterized by measuring physicochemical as well as photophysical properties. Here, standardized protocols and reference materials are needed to enable comparisons of results between research groups worldwide. The comparison of results in particular for photophysical characteristics of UCNPs is currently extremely challenging as evidenced by data shown in Table 1. For example, as discussed earlier, the QY_{UC} of UCNPs is dependent on the laser excitation power density. As shown in Table 1, there is currently no consensus in the community as to how to measure QY_{UC} (*e.g.*, absolute *versus* relative measurements; measurements at a single excitation power density *versus* measurement over the entire range of excitation power densities to determine saturation effects). Standardized protocols and reference materials are of great importance to

DOI: 10.1021/acsnano.7b07120
ACS Nano XXXX, XXX, XXX–XXX

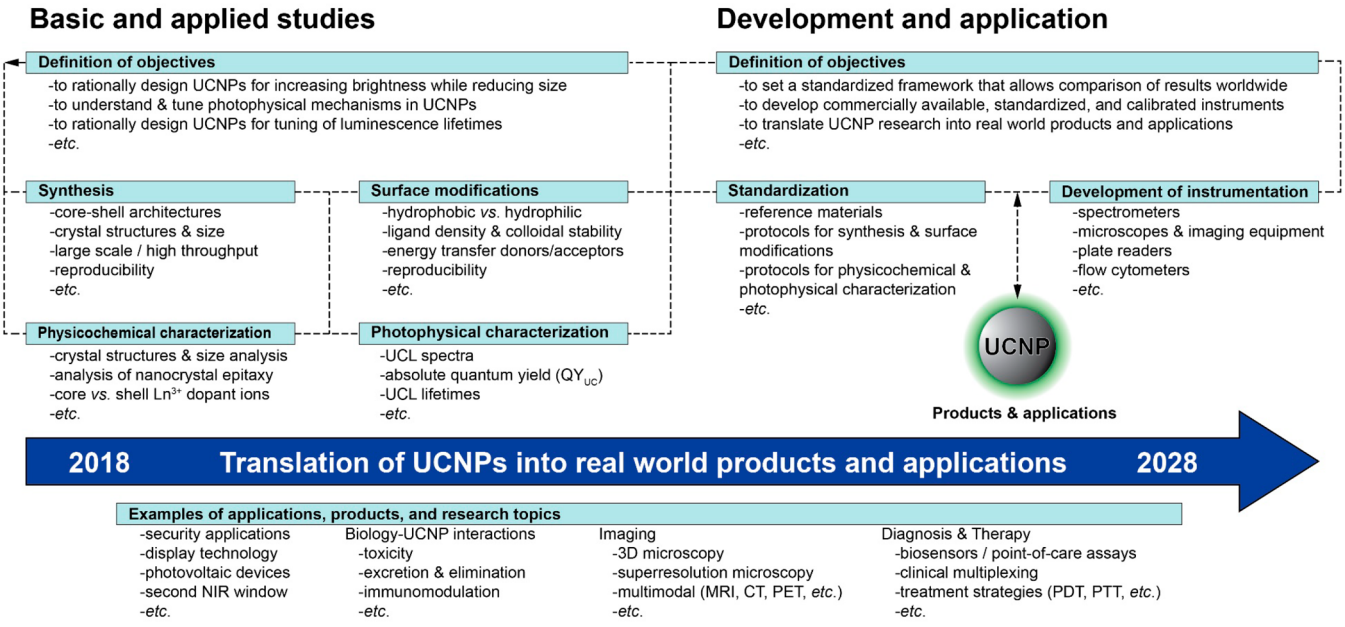

Figure 4. Proposal for a 10 year strategic plan of upconverting nanoparticle (UCNP) research. To further advance progress in the field of UCNP research, fundamental and applied studies are needed that address synthesis, surface modification, and characterization. Such studies might lead to the fabrication of reference materials and a definition of standardized protocols that would enable comparison of results from laboratories worldwide. With the development of commercially available instrumentation, this strategic plan might help facilitate the ultimate goal of UCNP research, that is, translation of UCNPs from the academic stage to a broad variety of real-world applications (*e.g.*, display technology, photovoltaic devices, sensors, biomedical diagnosis, and therapy). UCNP, upconverting nanoparticle; UCL, upconversion luminescence; Ln, lanthanide; NIR, near-infrared; 3D, three-dimensional; MRI, magnetic resonance imaging; CT, computed tomography; PET, positron emission tomography; PTT, photothermal therapy; PDT, photodynamic therapy.

build a foundation in the field by enabling the direct comparison of results. Beyond that, the development of commercial instrumentation is crucial for the successful translation of UCNPs into real-world applications. Instruments that are currently being used in UCNP research are mostly custom built because UCNPs require specialized excitation sources, such as continuous wave laser diodes, which are typically not available with commercial instruments. However, custom-built instruments are oftentimes not well characterized, for example in terms of laser excitation power density or laser beam profile, adding another layer of complexity when trying to compare results from different research groups. The development of commercial instrumentation (*e.g.*, spectrometers and microscopes) is a critical step and will be of great value to overcome challenges that the field is currently facing in terms of reproducibility and robustness of results. The interplay between synthesis, characterization, and development of standardized protocols, reference materials, and commercial instrumentation for UCNPs is a key feature to ensure translation.

Translation of UCNPs will be facilitated by the tremendous engineering flexibility that these types of nanomaterials offer. In bioanalytical and biomedical fields, the shift of the excitation wavelength to 800 nm was an important step to reduce overheating effects caused by the relatively strong absorption of water at 980 nm. This shift was achieved through advances in surface modification procedures and synthesis protocols that enabled precise control of multishell epitaxial nanocrystal architectures. The ability to fabricate multishell UCNP nanosystems opens the way for multimodal imaging probes and theranostic agents, for example, a combination of optical upconversion luminescence, magnetic resonance imaging (MRI), computed tomography (CT), positron emission tomography (PET), and photothermal and photodynamic therapy (PTT and PDT) within one single entity. In particular, the use of UCNPs for imaging and microscopy applications is highly promising. Jin and co-workers recently demonstrated that UCNPs can be used as labels in upconversion luminescence super-resolution nanoscopy. Using low-power super-resolution stimulated emission depletion (STED) microscopy, a resolution of 28 nm could be achieved upon 980 nm Gaussian laser excitation and 808 nm doughnut laser depletion of highly Tm^{3+} lanthanide ion doped $NaYF_4$(Yb/Tm) UCNPs.[27] Variations of lanthanide ion doping concentrations provides the additional benefit of tuning luminescence lifetimes of UCNPs to generate temporal-domain-based barcoding and encryption. Luminescence lifetime tuning can be exploited for bioanalytical and clinical multiplex assays as well as display technology and security applications.[28] In regard to the application of UCNPs for *in vivo* diagnostics and therapeutics, systematic fundamental research is needed to elucidate toxicological aspects of UCNPs.[29] Toxicological and immunological effects of UCNPs need to be assessed and pathways that will allow excretion and elimination of UCNPs from the body need to be explored. These investigations require collaboration of researchers from various disciplines, including chemistry, engineering, medicine, and biology.

Upconverting nanoparticle research is a multidisciplinary field that requires discussion, collaboration, and integration from academia as well as industry at the international level to help translate this technology into real-world applications. A great way to achieve this integration has been initiated by the European Cooperation in Science and Technology (COST) Action CM1403 through the European Upconversion Network: From the Design of Photon-Upconverting Nanomaterials to Biomedical Applications. This network sets a foundation for the coordination of basic and applied research to help advance

DOI: 10.1021/acsnano.7b07120
ACS Nano XXXX, XXX, XXX−XXX

UCNP technology toward translation. This initiative and the growing number of symposia and conferences that focus on UCNP research are important contributions for fostering collaborations and discussions in the field. Ultimately, a strategic plan as proposed in this Perspective combined with concerted efforts from researchers and industry partners worldwide may provide the rational groundwork for the translation of UCNPs from the academic stage into real-world products and applications.

AUTHOR INFORMATION

Corresponding Author

*E-mail: stefan.wilhelm@ou.edu.

ORCID

Stefan Wilhelm: 0000-0003-2167-6221

Notes

The author declares no competing financial interest.

ACKNOWLEDGMENTS

The author thanks Dr. T. Hirsch for fruitful discussions and manuscript proofreading.

REFERENCES

(1) Auzel, F. Upconversion and Anti-Stokes Processes with f and d Ions in Solids. *Chem. Rev.* **2004**, *104*, 139−173.

(2) Pollnau, M.; Gamelin, D. R.; Lüthi, S. R.; Güdel, H. U.; Hehlen, M. P. Power Dependence of Upconversion Luminescence in Lanthanide and Transition-Metal-Ion Systems. *Phys. Rev. B: Condens. Matter Mater. Phys.* **2000**, *61*, 3337−3346.

(3) Würth, C.; Kaiser, M.; Wilhelm, S.; Grauel, B.; Hirsch, T.; Resch-Genger, U. Excitation Power Dependent Population Pathways and Absolute Quantum Yields of Upconversion Nanoparticles in Different Solvents. *Nanoscale* **2017**, *9*, 4283−4294.

(4) Gargas, D. J.; Chan, E. M.; Ostrowski, A. D.; Aloni, S.; Altoe, M. V. P.; Barnard, E. S.; Sanii, B.; Urban, J. J.; Milliron, D. J.; Cohen, B. E.; Schuck, P. J. Engineering Bright Sub-10-nm Upconverting Nanocrystals for Single-Molecule Imaging. *Nat. Nanotechnol.* **2014**, *9*, 300−305.

(5) Rinkel, T.; Raj, A. N.; Dühnen, S.; Haase, M. Synthesis of 10 nm β-$NaYF_4$:Yb,Er/$NaYF_4$ Core/Shell Upconversion Nanocrystals with 5 nm Particle Cores. *Angew. Chem., Int. Ed.* **2016**, *55*, 1164−1167.

(6) Ostrowski, A. D.; Chan, E. M.; Gargas, D. J.; Katz, E. M.; Han, G.; Schuck, P. J.; Milliron, D. J.; Cohen, B. E. Controlled Synthesis and Single-Particle Imaging of Bright, Sub-10 nm Lanthanide-Doped Upconverting Nanocrystals. *ACS Nano* **2012**, *6*, 2686−2692.

(7) Rinkel, T.; Nordmann, J.; Raj, A. N.; Haase, M. Ostwald-Ripening and Particle Size Focussing of Sub-10 nm $NaYF_4$ Upconversion Nanocrystals. *Nanoscale* **2014**, *6*, 14523−14530.

(8) Wilhelm, S.; Kaiser, M.; Würth, C.; Heiland, J.; Carrillo-Carrion, C.; Muhr, V.; Wolfbeis, O. S.; Parak, W. J.; Resch-Genger, U.; Hirsch, T. Water Dispersible Upconverting Nanoparticles: Effects of Surface Modification on Their Luminescence and Colloidal Stability. *Nanoscale* **2015**, *7*, 1403−1410.

(9) Haase, M.; Schäfer, H. Upconverting Nanoparticles. *Angew. Chem., Int. Ed.* **2011**, *50*, 5808−5829.

(10) Han, S.; Deng, R.; Xie, X.; Liu, X. Enhancing Luminescence in Lanthanide-Doped Upconversion Nanoparticles. *Angew. Chem., Int. Ed.* **2014**, *53*, 11702−11715.

(11) Resch-Genger, U.; Gorris, H. H. Perspectives and Challenges of Photon-Upconversion Nanoparticles - Part I: Routes to Brighter Particles and Quantitative Spectroscopic Studies. *Anal. Bioanal. Chem.* **2017**, *409*, 5855−5874.

(12) Liu, G. Advances in the Theoretical Understanding of Photon Upconversion in Rare-Earth Activated Nanophosphors. *Chem. Soc. Rev.* **2015**, *44*, 1635−1652.

(13) Chen, G.; Damasco, J.; Qiu, H.; Shao, W.; Ohulchanskyy, T. Y.; Valiev, R. R.; Wu, X.; Han, G.; Wang, Y.; Yang, C.; Ågren, H.; Prasad, P. N. Energy-Cascaded Upconversion in an Organic Dye-Sensitized Core/Shell Fluoride Nanocrystal. *Nano Lett.* **2015**, *15*, 7400−7407.

(14) Fischer, S.; Bronstein, N. D.; Swabeck, J. K.; Chan, E. M.; Alivisatos, A. P. Precise Tuning of Surface Quenching for Luminescence Enhancement in Core−Shell Lanthanide-Doped Nanocrystals. *Nano Lett.* **2016**, *16*, 7241−7247.

(15) Muhr, V.; Würth, C.; Kraft, M.; Buchner, M.; Baeumner, A. J.; Resch-Genger, U.; Hirsch, T. Particle-Size-Dependent Förster Resonance Energy Transfer from Upconversion Nanoparticles to Organic Dyes. *Anal. Chem.* **2017**, *89*, 4868−4874.

(16) Li, Y.; Liu, X.; Yang, X.; Lei, H.; Zhang, Y.; Li, B. Enhancing Upconversion Fluorescence with a Natural Bio-Microlens. *ACS Nano* **2017**, DOI: 10.1021/acsnano.7b04420.

(17) Huber, A.; Behnke, T.; Würth, C.; Jaeger, C.; Resch-Genger, U. Spectroscopic Characterization of Coumarin-Stained Beads: Quantification of the Number of Fluorophores per Particle with Solid-State ^{19}F-NMR and Measurement of Absolute Fluorescence Quantum Yields. *Anal. Chem.* **2012**, *84*, 3654−3661.

(18) Muhr, V.; Wilhelm, S.; Hirsch, T.; Wolfbeis, O. S. Upconversion Nanoparticles: From Hydrophobic to Hydrophilic Surfaces. *Acc. Chem. Res.* **2014**, *47*, 3481−3493.

(19) Jiang, G.; Pichaandi, J.; Johnson, N. J. J.; Burke, R. D.; van Veggel, F. C. J. M. An Effective Polymer Cross-Linking Strategy To Obtain Stable Dispersions of Upconverting $NaYF_4$ Nanoparticles in Buffers and Biological Growth Media for Biolabeling Applications. *Langmuir* **2012**, *28*, 3239−3247.

(20) Dong, A.; Ye, X.; Chen, J.; Kang, Y.; Gordon, T.; Kikkawa, J. M.; Murray, C. B. A Generalized Ligand-Exchange Strategy Enabling Sequential Surface Functionalization of Colloidal Nanocrystals. *J. Am. Chem. Soc.* **2011**, *133*, 998−1006.

(21) Wilhelm, S.; del Barrio, M.; Heiland, J.; Himmelstoß, S. F.; Galbán, J.; Wolfbeis, O. S.; Hirsch, T. Spectrally Matched Upconverting Luminescent Nanoparticles for Monitoring Enzymatic Reactions. *ACS Appl. Mater. Interfaces* **2014**, *6*, 15427−15433.

(22) Zhan, Q.; Qian, J.; Liang, H.; Somesfalean, G.; Wang, D.; He, S.; Zhang, Z.; Andersson-Engels, S. Using 915 nm Laser Excited Tm^{3+}/Er^{3+}/Ho^{3+}- Doped $NaYbF_4$ Upconversion Nanoparticles for *in Vitro* and Deeper *in Vivo* Bioimaging Without Overheating Irradiation. *ACS Nano* **2011**, *5*, 3744−3757.

(23) Zou, W.; Visser, C.; Maduro, J. A.; Pshenichnikov, M. S.; Hummelen, J. C. Broadband Dye-Sensitized Upconversion of Near-Infrared Light. Nat. *Nat. Photonics* **2012**, *6*, 560−564.

(24) Shen, J.; Chen, G.; Vu, A.-M.; Fan, W.; Bilsel, O. S.; Chang, C.-C.; Han, G. Engineering the Upconversion Nanoparticle Excitation Wavelength: Cascade Sensitization of Tri-Doped Upconversion Colloidal Nanoparticles at 800 nm. *Adv. Opt. Mater.* **2013**, *1*, 644−650.

(25) Xie, X.; Li, Z.; Zhang, Y.; Guo, S.; Pendharkar, A. I.; Lu, M.; Huang, L.; Huang, W.; Han, G. Emerging ≈ 800 nm Excited Lanthanide-Doped Upconversion Nanoparticles. *Small* **2017**, *13*, 1602843.

(26) Chen, G.; Shao, W.; Valiev, R. R.; Ohulchanskyy, T. Y.; He, G. S.; Ågren, H.; Prasad, P. N. Efficient Broadband Upconversion of Near-Infrared Light in Dye-Sensitized Core/Shell Nanocrystals. *Adv. Opt. Mater.* **2016**, *4*, 1760−1766.

(27) Liu, Y.; Lu, Y.; Yang, X.; Zheng, X.; Wen, S.; Wang, F.; Vidal, X.; Zhao, J.; Liu, D.; Zhou, Z.; Ma, C.; Zhou, J.; Piper, J. A.; Xi, P.; Jin, D. Amplified Stimulated Emission in Upconversion Nanoparticles for Super-Resolution Nanoscopy. *Nature* **2017**, *543*, 229−233.

(28) Lu, Y.; Zhao, J.; Zhang, R.; Liu, Y.; Liu, D.; Goldys, E. M.; Yang, X.; Xi, P.; Sunna, A.; Lu, J.; Shi, Y.; Leif, R. C.; Huo, Y.; Shen, J.; Piper, J. A.; Robinson, J. P.; Jin, D. Tunable Lifetime Multiplexing using Luminescent Nanocrystals. Nat. *Nat. Photonics* **2013**, *8*, 32−36.

(29) Gnach, A.; Lipinski, T.; Bednarkiewicz, A.; Rybka, J.; Capobianco, J. A. Upconverting Nanoparticles: Assessing the Toxicity. *Chem. Soc. Rev.* **2015**, *44*, 1561−1584.

(30) Phan, T. G.; Bullen, A. Practical Intravital Two-Photon Microscopy for Immunological Research: Faster, Brighter. *Immunol. Cell Biol.* **2010**, *88*, 438−444.

DOI: 10.1021/acsnano.7b07120
ACS Nano XXXX, XXX, XXX−XXX

(31) Pokhrel, M.; Kumar, G. A.; Sardar, D. K. Highly Efficient NIR to NIR and VIS Upconversion in Er^{3+} and Yb^{3+} doped in M_2O_2S (M = Gd, La, Y). *J. Mater. Chem. A* **2013**, *1*, 11595.
(32) Pokhrel, M.; Gangadharan, A.; Sardar, D. K. k.; Sardar, D. K. High Upconversion Quantum Yield at Low Pump Threshold in Er^{3+}/Yb^{3+} doped La_2O_2S phosphor. *Mater. Lett.* **2013**, *99*, 86−89.
(33) Boyer, J.-C.; van Veggel, F. C. J. M. Absolute Quantum Yield Measurements of Colloidal $NaYF_4$: Er^{3+}, Yb^{3+} Upconverting Nanoparticles. *Nanoscale* **2010**, *2*, 1417−1419.
(34) Page, R. H.; Schaffers, K. I.; Waide, P. A.; Tassano, J. B.; Payne, S. A.; Krupke, W. F.; Bischel, W. K. Upconversion-Pumped Luminescence Efficiency of Rare-Earth-Doped Hosts Sensitized with Trivalent Ytterbium. *J. Opt. Soc. Am. B* **1998**, *15*, 996.
(35) Liu, H.; Xu, C. T.; Lindgren, D.; Xie, H.; Thomas, D.; Gundlach, C.; Andersson-Engels, S. Balancing Power Density Based Quantum Yield Characterization of Upconverting Nanoparticles for Arbitrary Excitation Intensities. *Nanoscale* **2013**, *5*, 4770−4775.
(36) Huang, P.; Zheng, W.; Zhou, S.; Tu, D.; Chen, Z.; Zhu, H.; Li, R.; Ma, E.; Huang, M.; Chen, X. Lanthanide-Doped $LiLuF_4$ Upconversion Nanoprobes for the Detection of Disease Biomarkers. *Angew. Chem., Int. Ed.* **2014**, *53*, 1252−1257.
(37) Wilhelm, S. Perspectives of Upconverting Luminescent Nanoparticles for (Bio)-Analytical Applications. Ph.D. Dissertation; University of Regensburg, Regensburg, 2015.
(38) Liu, Q.; Sun, Y.; Yang, T.; Feng, W.; Li, C.; Li, F. Sub-10 nm Hexagonal Lanthanide-Doped $NaLuF_4$ Upconversion Nanocrystals for Sensitive Bioimaging in Vivo. *J. Am. Chem. Soc.* **2011**, *133*, 17122−17125.
(39) Li, X.; Shen, D.; Yang, J.; Yao, C.; Che, R.; Zhang, F.; Zhao, D. Successive Layer-by-Layer Strategy for Multi-Shell Epitaxial Growth: Shell Thickness and Doping Position Dependence in Upconverting Optical Properties. *Chem. Mater.* **2013**, *25*, 106−112.
(40) Xu, C. T.; Svenmarker, P.; Liu, H.; Wu, X.; Messing, M. E.; Wallenberg, L. R.; Andersson-Engels, S. High-Resolution Fluorescence Diffuse Optical Tomography Developed with Nonlinear Upconverting Nanoparticles. *ACS Nano* **2012**, *6*, 4788−4795.
(41) Chen, G.; Shen, J.; Ohulchanskyy, T. Y.; Patel, N. J.; Kutikov, A.; Li, Z.; Song, J.; Pandey, R. K.; Agren, H.; Prasad, P. N.; Han, G. (α-$NaYbF_4$:Tm^{3+})/CaF_2 Core/Shell Nanoparticles with Efficient Near-Infrared to Near-Infrared Upconversion for High-Contrast Deep Tissue Bioimaging. *ACS Nano* **2012**, *6*, 8280−8287.

DOI: 10.1021/acsnano.7b07120
ACS Nano XXXX, XXX, XXX−XXX